# Chapter 7 ESTIMATE OF GEOSTROPHIC CURRENTS

## *7.1 The Geostrophic Model*

An important feature of the response of a rotating fluid to gravity is that it does not adjust to a state of rest, but to an equilibrium state named as “geostrophic” by Shaw in 1916 (Gill, 1983).

The geostrophic equilibrium results from the balance between the horizontal pressure gradient forces and the Coriolis force, and therefore implies neglecting other forces such as tidal forces and friction. The pressure gradient force is due to both, variations in the density field (which depends on the salinity, temperature and pressure, $r = r(S,T,p)$) and differences in sea level (which arise by the effect of wind stress and also by the presence of continents, which often produce a piling up effect when a flow impinges against the shore). The Coriolis force is due to the rotation of the earth at a constant angular velocity $\Omega = 7.20x10^{-5}\,\mathrm{sec}^{-1}$.

A difference in pressure between two nearby points over a level plane (*z=const*) tends to be compensated (i.e., the ocean pressure field tends to become horizontal), but soon after a water parcel starts to move from high to low pressure it ''feels'' the effects of the rotation of the earth, which deviates its motion to the right (left) in the northern (southern) hemisphere until the pressure gradient acceleration is exactly compensated by the Coriolis acceleration. From that point, the steady state geostrophic current is maintained.

It is important to realize that the assumptions underlying the geostrophic balance (basically the dominance of the pressure and Coriolis accelerations compared to friction and centripetal accelerations) are valid for a large range of scales including the large scale (> 100 km) and most of the mesoscale (10-100 km). [ In fact, both the ocean and the atmosphere tend to approach the state of geostrophic equilibrium all the time, as it represents a minimum for the total energy involved (Gill, 1983). ] This allows to estimate a large fraction of the dominant currents in the ocean from vertical profiles of temperature and salinity,

such as those measured with CTDs. A complete explanation can be found in classical physical oceanography textbooks such as Gill (1983) and Pond and Pickard (1978). The basic aspects of the approximation will nevertheless be summarized for the sake of completeness.

The equations, in their simplest form are:

$$fu = -r^{-1}\,\partial p/\partial y \qquad \textbf{(7.1)}$$
$$fv = r^{-1}\,\partial p/\partial x$$

where $f = 2\Omega\sin q$ represents the Coriolis term, which depends on the latitude $q$, $(u,v)$ are the geostrophic velocity components, which flow along contours of constant pressure, and $(\partial p/\partial x, \partial p/\partial y)$ are the horizontal pressure gradients.

In the ocean, density is computed from values of temperature, salinity and pressure using an empirical equation of state. For practical reasons, instead of computing the pressure field on level (*z=const*) surfaces, the height of prescribed isobaric surfaces is computed, either in the form of geopotential or dynamic height. The geopotential $\Phi$ is related to the amount of work done (or gain in potential energy) when raising a mass **M** a vertical distance **dz** against the gravity force,

$$Md\Phi = Mgdz$$

or

$$d\Phi = gdz \qquad \text{(Joules Kg}^{-1} = \text{m}^2\text{s}^{-2}\text{)}.$$

To estimate $\Phi$, the density is represented in terms of the specific volume anomaly $d$, defined as the actual specific volume $v_s = r^{-1}$ minus the specific volume of a water parcel submitted to same pressure but at a temperature of 0 °C and salinity of 35.

This is,

$$d = v_s(S,T,p) - v_s(35,0,p) \qquad \textbf{(7.2)}$$

Using the hydrostatic equation, the geopotential at one pressure $p_1$ level relative to another $p_2$, is simply given by

$$\Delta\Phi = \Phi_2 - \Phi_1 = -\int_{p_1}^{p_2} d\,dp \qquad \textbf{(7.3)}$$

In practical oceanography, the geopotential is usually replaced by Dynamic Height (DH), which only differs from the latter in a factor of 10 (1 dyn m = 10 J kg$^{-1}$).

Geostrophic velocities at pressure $p_1$ relative to $p_2$ can therefore be estimated from (7.1) and (7.3), rendering

$$\begin{aligned} -f\{v(p_1) - v(p_2)\} &= -\frac{\partial}{\partial x}\{\Phi(p_1) - \Phi(p_2)\} \\ f\{u(p_1) - u(p_2)\} &= -\frac{\partial}{\partial y}\{\Phi(p_1) - \Phi(p_2)\} \end{aligned} \qquad \textbf{(7.4)}$$

It is worth stressing that (7.4) does not provide absolute velocities at the isobaric level p1, but the velocity shear with respect to level p2 (referred to as “reference level”). Absolute velocities can only be obtained if the velocity field at p2 is known (e.g. from direct measurements) or p2 can be considered as a no-motion level. A common practice is to take a deep reference level, where current velocities are assumed to be much smaller than at upper levels and therefore shear velocities approach absolute velocities.

Another shortcoming of the method appears when the selected reference level reaches the ocean bottom as the stations get closer to the shore, as it is the case in the Ebro Delta shelf/slope region. At first, the presence of the bottom might seem to simplify the problem, since it is indeed a surface below which no motion is possible. However, geostrophic velocities can only be obtained from the dynamic height distribution on isobaric surfaces, and the sea bottom does usually not follow such surfaces. Therefore, some kind of

assumption on the contribution to the dynamic height “below the bottom” (down to the reference level) is needed in shallow regions.

In this chapter we compare two different methods aimed to estimate a dynamic field below the sea bottom, namely:

a) the method proposed by Csanady (1979), and

b) the use of Empirical Orthogonal Functions as an extrapolation procedure, as suggested by Pedder and Gomis (1997).

### *7.2 Csanady’s Method*

The original work by Csanady (1979) was aimed to estimate the along-shore and across-shore pressure gradients on the western margin of the North Atlantic, from Cape Hatteras to Halifax. The proposed solution takes into account the effects of stratification (unlike a previous model proposed by himself), and the basic assumption is that major density variations over shelf-slope regions occur across isobaths. The reason is twofold: first, the freshwater input at the shore or preferential heating of shallow waters; second, geostrophic adjustment of the density field to predominantly along-isobath flow makes that isopycnals are tilted in an across isobath section, bending towards the bottom. The Csanady method actually assumes along-isobath density variations to vanish, and considers the problem of the surface elevation field that is induced by a uniform density along a long coastline.

After some further simplifying assumptions it is obtained:

$$V = -\int_{H_m}^{0} \boldsymbol{e} \cdot dz\,, \qquad \textbf{(7.5)}$$

where $V$ is the sea level height, $e$ is a “perturbation density” relative to deep water density ( $r = r_0(1+e(x,z))$ ) and $H_m$ is the reference depth of no motion. In this form, equation (7.5) is equivalent to the steric setup field, itself a physically reasonable generalization of the dynamic height concept, valid for

coastal regions of simple geometry and simple density distribution. The path of integration is along the sea floor and perpendicular to the coast, from deep to shallow water as shown in Figure 7-1.

To perform the step-wise vertical integration of Figure 7-1, the dynamic height is first calculated at 10 m intervals taking as reference level the level located immediately below. The values obtained in this way are usually referred to as ***thickness***, since they give a measure of the layer thickness. Dynamic height can then be estimated as the sum of successive thickness values, and here it will be referred to as ***dynamic thickness***. If the bottom depth is larger or equal to 500 m, dynamic thickness will be equivalent to dynamic height. On the shelf/slope domain (where the bottom depth is shallower than 500 m), dynamic thickness will depend on the model used to extrapolate the thickness profile below the bottom.

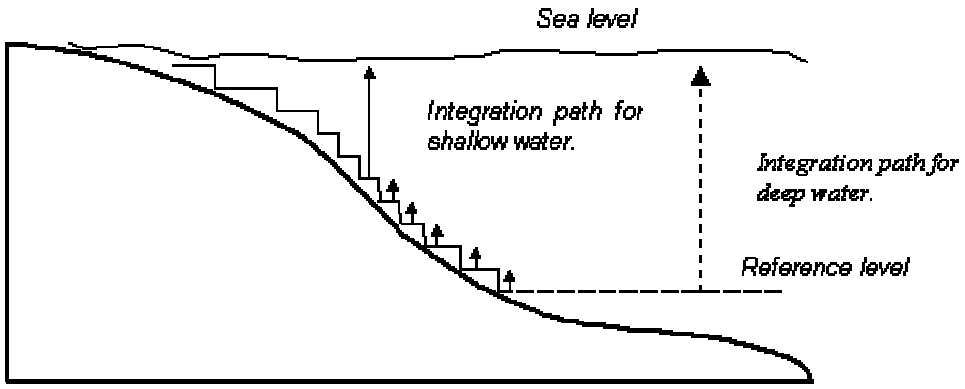


**Figure 7-1 Schematization of the integration path proposed by Csanady for the dynamic height estimates in shallow regions.**

For Csanady's method, thickness values at 10 m intervals were first derived from CTD profiles and then projected onto the grid with the successive corrections method. Obviously, as the depth increases, the number of CTD casts whose data can be used to generate the 2D grid at a given level decreases. Once the 2D grids are generated, a "3D" thickness grid can be created simply by overlapping the set of 2D grids. Dynamic thickness can then be estimated in shallow regions following the integration path shown above (along transects perpendicular to the shore). The geostrophic current is finally calculated from the dynamic thickness field.

### *7.3 Results with Csanady's Method.*

As in the previous sections we will show the results for the FANS III, FANS II, FANS I and MEGO 94 campaigns. For each of them, we will present one figure with 6 frames. The DT contour distributions will always be on the left column, and their associated geostrophic currents on the right. The rows, from top to bottom, correspond to results at 10, 50 and 100 m.

#### 7.3.1 FANS III

The results for this campaign are summarized in Figure 7-2. A first worth noting feature common to all depths is a south-westward flow adjacent to the open ocean boundary and located in the southern half of the domain. More to the north there is an incoming flow across the open ocean boundary, which at 10 m seems to turn in a cyclonic path with velocities lower than 10 $^{m}/_{s}$. At 50 and 100 m, this eastern flow is stronger than at 10 m (around 15 $^{cm}/_{s}$), and clearly continues towards the northern boundary, where most of it leaves the domain, and a small part flows towards the coast.

The circulation on the upper shelf ($H_b$ < 100 m) has a suspicious distribution, with velocities that have a strong component in the along-transect direction (very evident at 50 m). The magnitude of the v-component (perpendicular to the coast) is of the order of 30 $^{cm}/_{s}$. The same feature is also clearly observed in the DT distributions between the Ebro Delta and the northern boundary.

At 10 m, the geostrophic currents are slightly less transect-oriented, particularly around the Ebro Delta, where a cyclonic circulation is clearly observed. While these flow structures are real, in the sense that reflect the uppermost thickness layers contribution, they must be strongly contaminated by the spurious along-transect circulation at deeper levels.

#### 7.3.2 FANS II

Usually the northern current is enhanced during the winter months as a consequence of the sharpening of density gradients. The latter become stronger as the continental fresh water supply increases through rain. The

current is particularly intense on the slope and open ocean domains (Figure 7-3), with highest south-westward velocity components of nearly 38 $^{cm}/_{s}$ at 10 m, 35.5 $^{cm}/_{s}$ and 31.5 $^{cm}/_{s}$ at 50 and 100 m respectively. It shifts direction forced by the widening of the shelf, and the limited extension of the study domain does not allow to cover its whole influence region south of the Ebro Delta.

On the other hand, a gyre structure is insinuated close to the northern boundary, just west of the northern current. The data reveal the presence of this eddy in the northernmost transversal sections of salinity and density.

While the two above mentioned aspects of the geostrophic circulation are supported by data, the upper shelf domain results show unreal along-transect velocities, as in FANS III. Most of the velocity vectors are lower than 10 $^{cm}/_{s}$, but there is a critical nod around 1.35º E, 40.7º N where the DT contours show a sharper gradient, which results in along-transect velocities close to 30 $^{cm}/_{s}$.

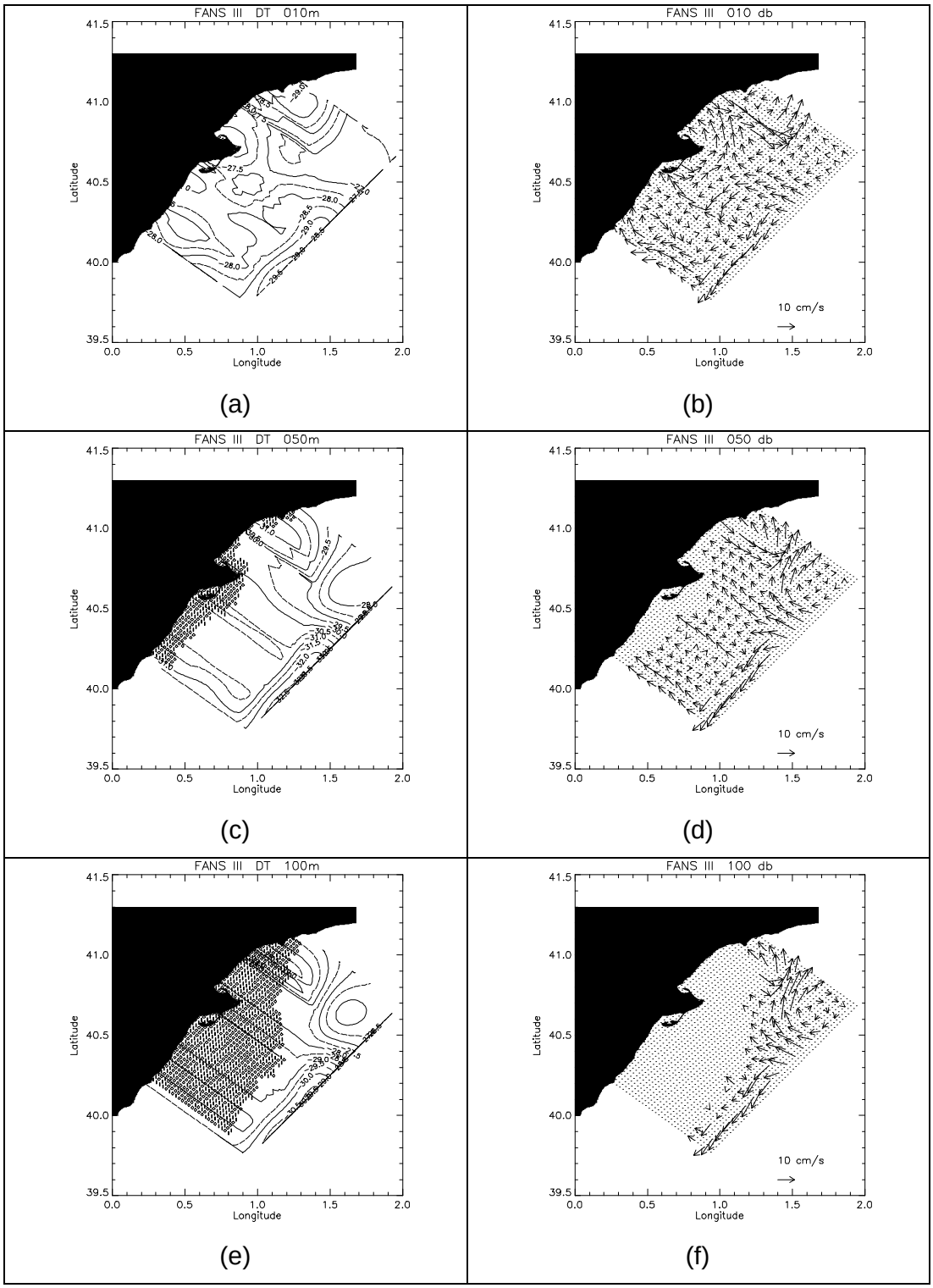


**Figure 7-2 FANS III Dynamic thickness, in dyn cm (left column), and geostrophic currents (right column) following Csanady's method at three different depths: 10 m (a, b), 50 m (c, d) and 100 m (e, f).**

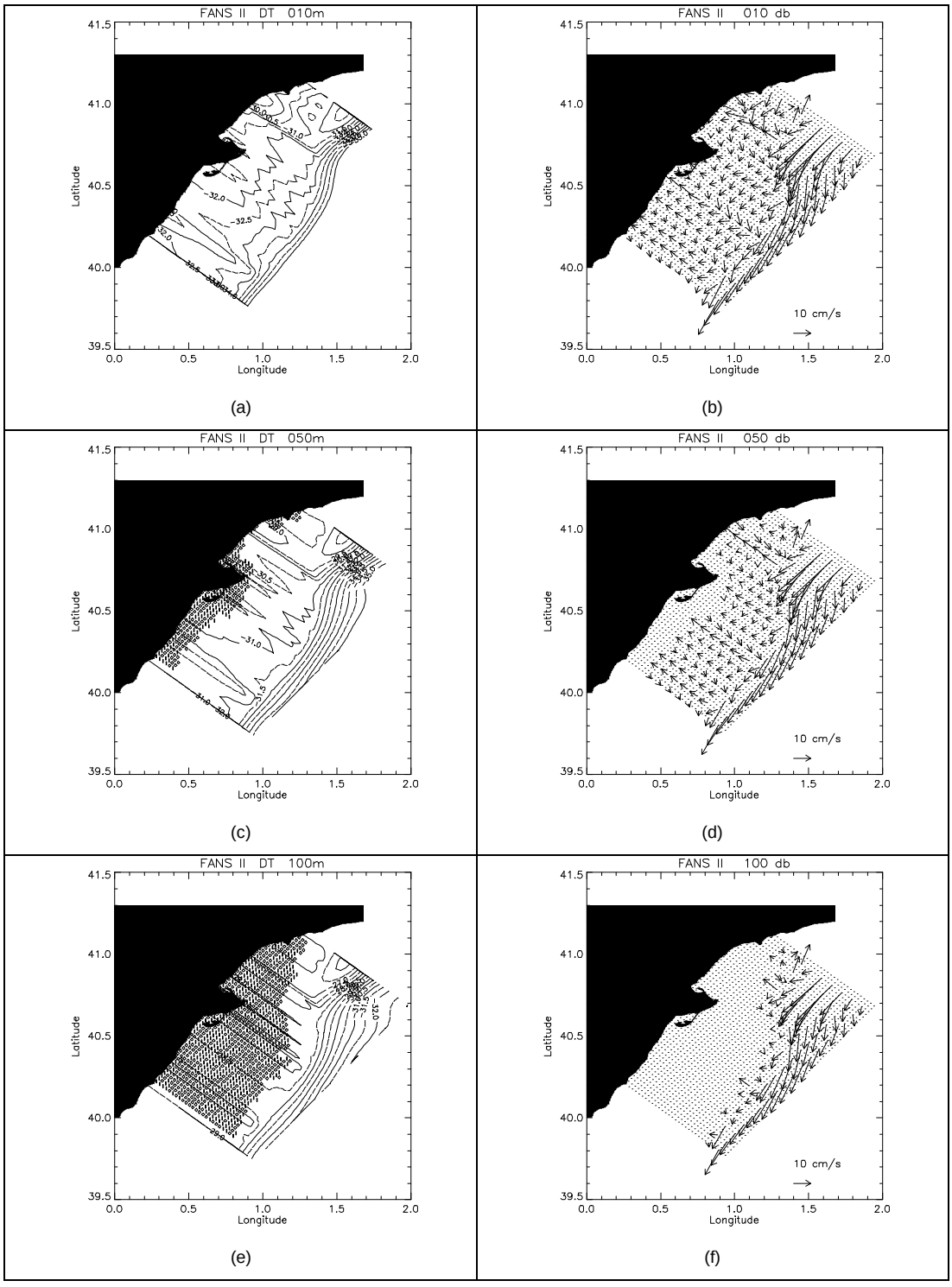


**Figure 7-3 FANS II Dynamic thickness, in dyn cm (left column), and geostrophic currents (right column) following Csanady's method at three different depths: 10 m (a, b), 50 m (c, d) and 100 m (e, f).**

### 7.3.3 FANS I

The geostrophic circulation (Figure 7-4) on the outer slope and open ocean regions, is characterised by a flow exiting through the eastern boundary. At 10 m, there is an anticyclonic eddy at the north-eastern side of the domain, with incoming velocities slightly larger than 10 $^{cm}/_{s}$. Just west of this eddy, there is another incoming flow through the northern boundary that flows around the eddy and turns south, forced perhaps by the bathymetry. This flow leaves the domain through the eastern boundary. South of the Ebro Delta there appears a south-eastwards flow, which would carry shelf waters across the slope into the open ocean. While the extent of this flow appears unreasonable (all across the shelf and slope, up to the open sea), it might in fact reflect a real feature, since it is also suggested in deep regions, where the vertical integration is straightforward. Finally, a cyclonic current is observed around the Ebro Delta. Unfortunately, also this signal appears to be contaminated by the along-transect flow components on the shelf.

At 50 and 100 m, the southward and south-westward geostrophic currents entering through the northern boundary are also visible, with slightly smaller velocities. The flow across the shelf, south of the Ebro Delta, is also apparent at 50 m and suggested at 100 m.

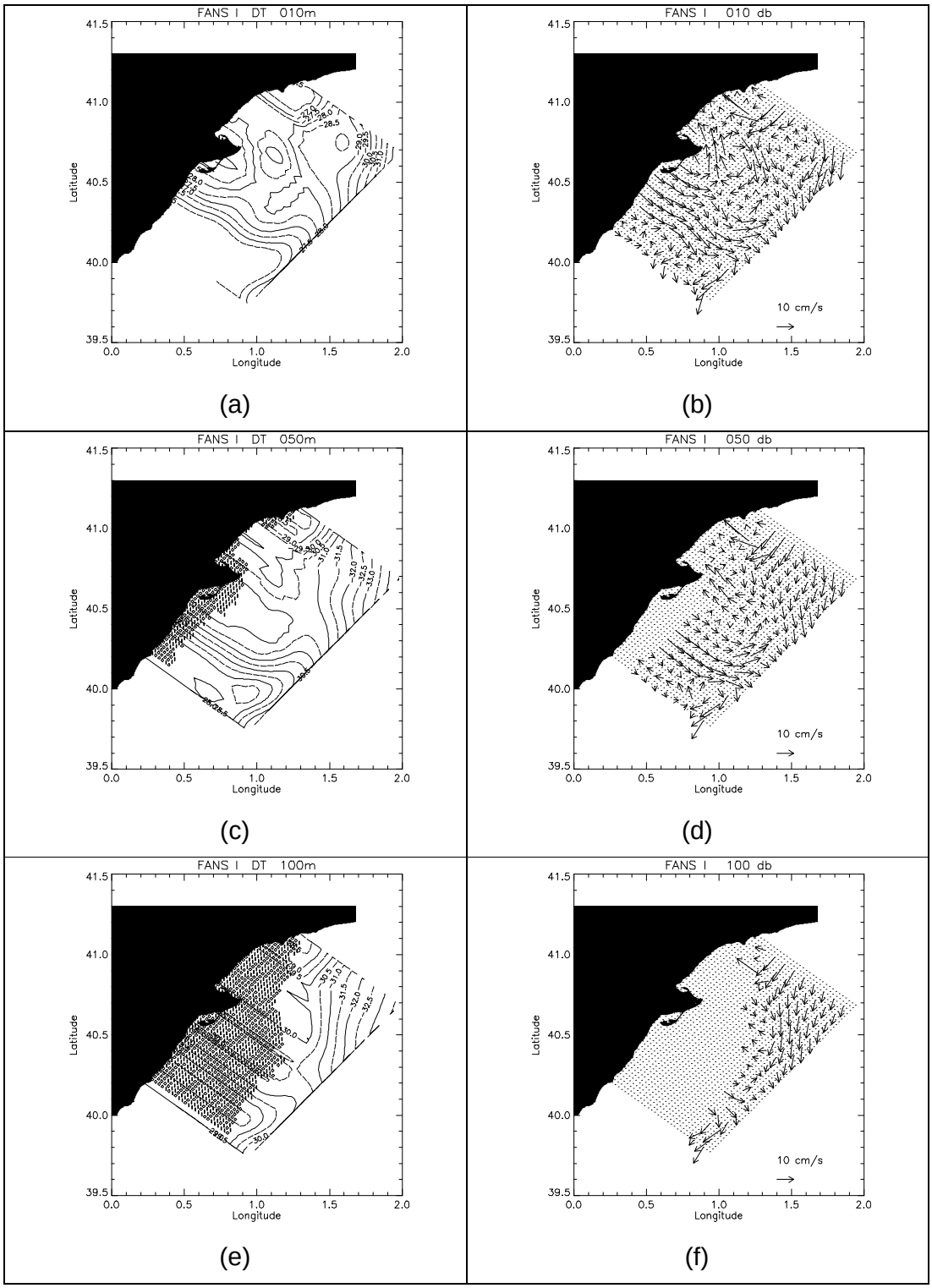


**Figure 7-4 FANS I Dynamic thickness, in dyn cm (left column), and geostrophic currents (right column) following Csanady's method at three different depths: 10 m (a, b), 50 m (c, d) and 100 m (e, f).**

### 7.3.4 MEGO 94

The homogeneous conditions that characterized the MEGO 94 campaign also reflects on the DT distribution and the geostrophic circulation (Figure 7-5), which show very little structure except in the open ocean areas. An eddy structure is partially detected at the north-eastern corner, with associated eastward and south-eastward velocities around 15 $^{cm}/_{s}$. South of it, and also on the open ocean border, a south-westward flow reaches 20 $^{cm}/_{s}$. This flow could also be associated with an eddy-like structure with cyclonic circulation.

The rest of the domain has little structure, with predominance of along-transect, low speed velocities.

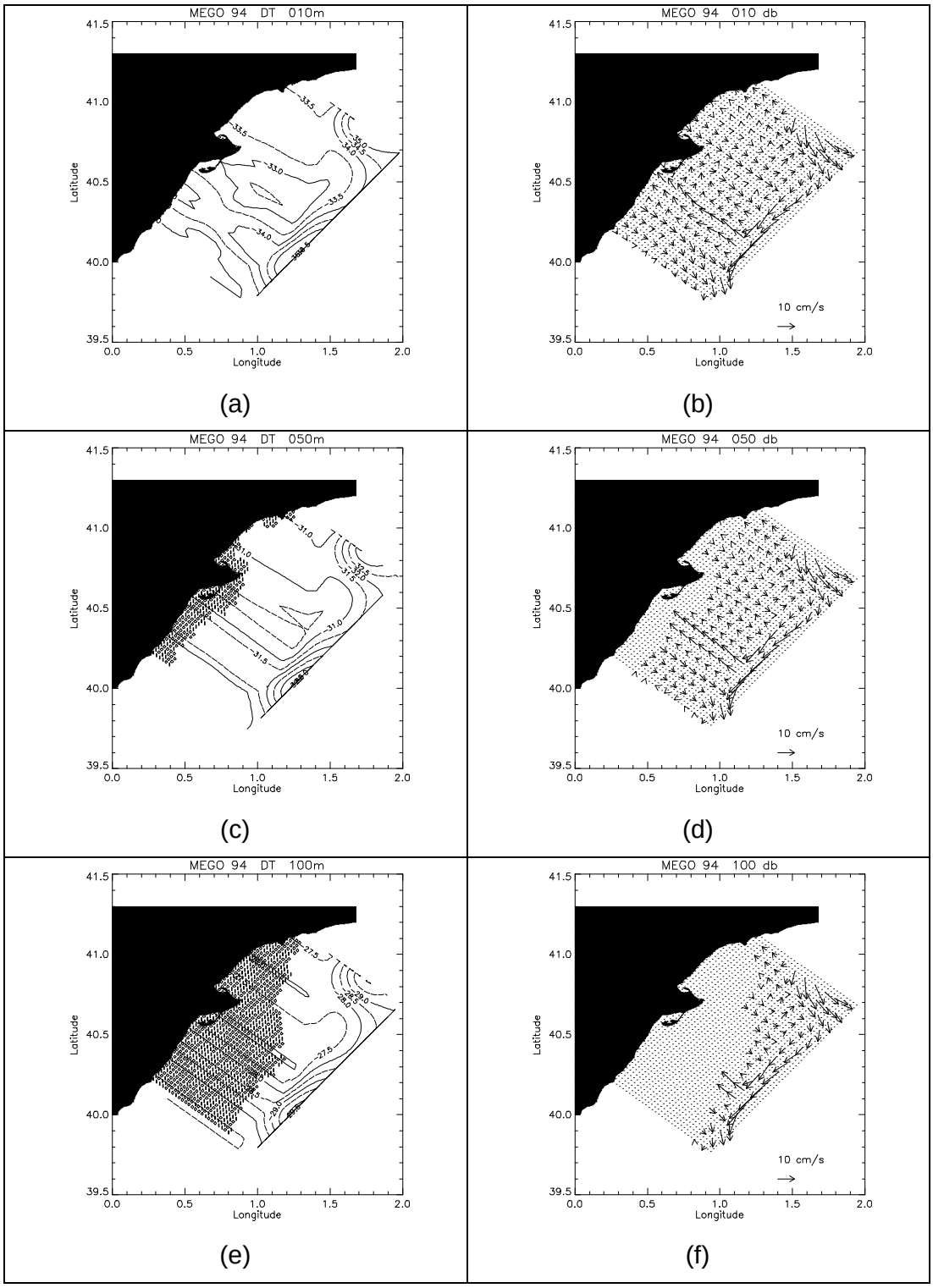


**Figure 7-5 MEGO 94 Dynamic thickness, in dyn cm (left column), and geostrophic currents (right column) following Csanady's method at three different depths: 10 m (a, b), 50 m (c, d) and 100 m (e, f).**

### 7.3.5 Csanady's method on an Analytic Thickness distribution

Because the obtained DT distributions on the shelf have shown spurious, along-transect velocities, we tested the method with an analytic 3D thickness distribution with constant values along the x-grid axis, and linearly variable on y. The thickness values at each grid point ( $x_g, y_g, z_g$ ) were defined according to

$$Th(x_g, y_g, z_g) = \langle Th(z_g) \rangle \left(1 + m y_g\right) \qquad \textbf{( 7-6)}$$

where m is a constant and the term $\langle Th(z_g) \rangle$ represents an average thickness profile. We chose it to be the mean profile of FANS II, since for that campaign the results provided by Csanady's method did show very clear along-transect velocities at all depth levels. With $m$ values of the order of 0.01, the DT distribution at 10 m has numerical values similar to the actual campaign data at 10 m, though the distribution does not resemble the campaign.

With the 3D thickness grid data defined in this way, we proceeded to compute the DT field following Csanady's vertical integration path over the actual Ebro Delta shelf/slope bathymetry. Results show again spurious along-transect (v-) velocities which are even higher than the simulated u-component. While $u_g$ ranges from –3.1 $^{cm}/_{s}$ to –0.02 $^{cm}/_{s}$ at 10 m, $v_g$ has values that range from –4.7 to 1.9 $^{cm}/_{s}$. These values vary only slightly for the levels shown, but the v-component is always higher.

If other slope values are used, the equivalent DT contour distribution results with other numerical values, and the geostrophic currents vary likewise.

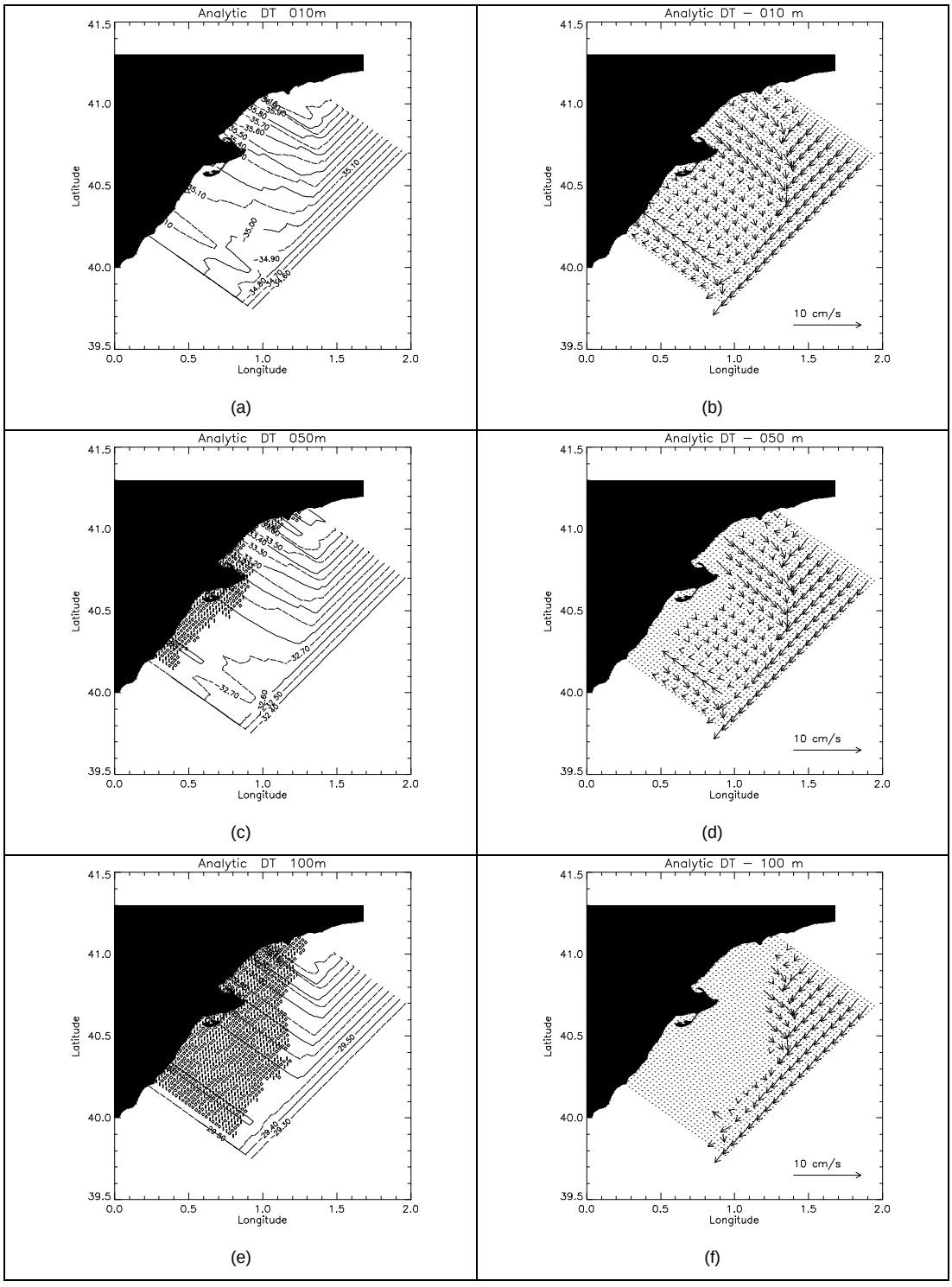


**Figure 7-6 Dynamic Thickness, in dyn cm, and geostrophic currents at 10, 50 and 100 m that result from the analytic linear thickness distribution, with m=0.01. The vertical integration on the shallow shelf/slope areas was performed following Csanady's methodology.**